

## Research Article

Mohamed Bechir Ben Hamida, Abdellatif M. Sadeq\*, Soundhar Arumugam, Palaniyappan Karuppusamy, Thulasidhas Dhilipkumar, Karthik V. Shankar, Murugan Rajesh and Nashmi Alrasheedi\*

# Evaluating the influence of graphene nano powder inclusion on mechanical, vibrational and water absorption behaviour of ramie/abaca hybrid composites

<https://doi.org/10.1515/ntrev-2025-0245>

Received July 4, 2025; accepted October 21, 2025;

published online December 8, 2025

**Abstract:** The present study examines the impact of incorporating graphene nanoparticles on the mechanical, vibrational, and moisture resistance properties of hybrid composites (HC) reinforced with ramie/abaca fibres. The composites were produced using compression moulding, with graphene dispersed in distinct concentrations (0.5, 1.0, and 1.5 wt%) in the epoxy matrix through ultrasonic sonication. The sample with 1.5 wt% graphene exhibited the highest performance, attaining a tensile strength (TS) of 22 MPa and a modulus of 3,116.897 MPa, representing increases of 175 % and 93.77 %, respectively, over the neat composites. The flexural strength also reached 70.64 MPa,

showing a 139.29 % improvement. Increasing the graphene content to 1.0 wt% (RA1.0) resulted in an impact strength of 4.69 J, a 94.60 % improvement over the neat composite. Atomic force microscopy (AFM) and Field emission scanning electron microscopy (FESEM) were used to examine the microstructure of HC. In free vibration analysis, the composite with 1.5 wt% graphene recorded the highest natural frequencies, indicating greater stiffness and less energy dissipation. The Shore D hardness increased with graphene content, reaching a peak of 82.2 at 1.5 wt% graphene inclusion. Water absorption reduced from 14.1 % in the unmodified composite to 10.8 % with 1.5 wt% graphene, demonstrating enhanced moisture resistance. Integrating 1.5 wt% graphene significantly improves the mechanical strength, stiffness, surface hardness, and moisture resistance of ramie/abaca HC, making it suitable for weight-sensitive applications in automotive, marine, and aerospace sectors.

**\*Corresponding authors: Abdellatif M. Sadeq**, Independent Researcher, Mechanical Engineering, Doha, Qatar, E-mail: [abdellatifsadeq23@gmail.com](mailto:abdellatifsadeq23@gmail.com). <https://orcid.org/0000-0002-0654-7774>; and **Nashmi Alrasheedi**, College of Engineering, Imam Mohammad Ibn Saud Islamic University (IMSIU), Riyadh, Saudi Arabia, E-mail: [nhrasheedi@imamu.edu.sa](mailto:nhrasheedi@imamu.edu.sa)

**Mohamed Bechir Ben Hamida**, Deanship of Scientific Research, Imam Mohammad Ibn Saud Islamic University (IMSIU), Riyadh, Saudi Arabia. <https://orcid.org/0000-0002-3128-4443>

**Soundhar Arumugam**, Department of Mechanical Engineering, Vel Tech Rangarajan Dr. Sagunthala R&D Institute of Science and Technology, Chennai 600062, Tamil Nadu, India, E-mail: [soundhar1372214@gmail.com](mailto:soundhar1372214@gmail.com)

**Palaniyappan Karuppusamy**, Department of Chemistry, Centre for Research and Development, Vinayaka Mission's Kirupananda Variyar Engineering College, Vinayaka Mission's Research Foundation (DU), Salem-636308, Tamil Nadu, India, E-mail: [karuppusamy98422@gmail.com](mailto:karuppusamy98422@gmail.com). <https://orcid.org/0000-0003-4406-5917>

**Thulasidhas Dhilipkumar and Karthik V. Shankar**, Department of Mechanical Engineering, Amrita Vishwa Vidyapeetham, Amritapuri, India; and Centre for Flexible Electronics and Advanced Materials, Amrita Vishwa Vidyapeetham, Amritapuri, India

**Murugan Rajesh**, School of Mechanical Engineering, Vellore Institute of Technology, Vellore, India. <https://orcid.org/0000-0001-9350-7756>

**Keywords:** graphene; hybrid composite; free vibration

## 1 Introduction

Polymer composites have become crucial in specialised applications over the past few decades, ranging from sports to biomedicine and defence. The transportation (aerospace and automotive), leisure, sports, and construction sectors are dominated by composites derived from synthetic fibres such as aramid, carbon, and Kevlar [1–3]. Since synthetic fibres are affordable and possess good mechanical performance, they are widely used across industries. However, these synthetic fibres have several drawbacks, including increased health risks, high energy consumption, elevated CO<sub>2</sub> emissions, non-renewability, recyclability issues, and non-biodegradability [4]. When petroleum-based materials are burned, a substantial amount of CO<sub>2</sub> is released into the atmosphere. Consequently, natural fibres (NFs) are now primarily replacing

petroleum-based fibres because of environmental concerns, sustainability, and the demand for biodegradable and energy-efficient products. Examples include banana, abaca, sisal, bamboo, pineapple, kenaf, luffa cylindrica, flax, coir, jute, vakka, palm, and ramie fibre [5–7]. The main components of NFs are cellulose, lignin, pectin, and hemicellulose. Compared to synthetic fibres, NFs offer several advantages, including low cost, lightweight nature, availability, biodegradability, recyclability, ease of processing, reduced health risks, improved wear resistance, corrosion resistance, and excellent load-bearing capacity [8]. However, NFs do have limitations, including lower flame resistance, poor interfacial adhesion between the matrix and reinforcement, reduced durability, water resistance issues, and variability in quality and cost [9]. The poor bonding strength in NFs composite mainly results from weak interface interactions between the fibre and the matrix [10]. Surface treatments aim to replace conventional carbonyl and hydroxyl groups with new interfacial compounds that enhance adhesion with the polymer matrix. To enhance the bonding between fibres and the matrix, NFs are commonly treated with various chemical agents, including alkalis, permanganates, chlorites, stearic acid, benzoyl compounds, and peroxides [11–13]. An HC is composed of two or more different fibre types, where one type addresses the weaknesses of the other. Hybridization allows designers to tailor material properties to specific requirements [14]. Dhandapani and Magalingam (2021) conducted a study on sisal/palm fibre reinforced HC. Their results exhibited that a HC with 35 % sisal/palm fibre demonstrated improved TS (0.63 %), flexural strength (22.62 %), and impact strength (36.59 %) compared to other combinations [15]. Anandraj et al. (2022) fabricated HC with various stacking sequences of hemp, abaca, Kevlar, and glass fibre. The Kevlar/abaca composite exhibited superior mechanical properties compared to other combinations [16]. Suriyaprakash et al. developed HC reinforced with epoxy, consisting of ramie-hemp and coconut shell particles. Their findings showed that 28 % ramie-hemp and 2.0 wt% coconut shell particles offered superior tensile, flexural, and impact properties compared to other formulations [17]. Sivasankar et al. prepared HC using abaca and hemp fibres in varying weight ratios. Their study suggested that a 30:10 ratio of abaca to hemp provided better tensile and flexural strength than other combinations [18]. Sumesh et al. prepared hybrid ramie/flax epoxy composites via compression moulding. Results showed that 40 wt% ramie/flax and fibre lengths of 1 cm yielded enhanced properties compared to other configurations [19]. Arumugam et al. investigated the impact of chitosan accumulation on glass fibre/sisal fibre hybrid sandwich composites, concluding that incorporating chitosan significantly enhanced both mechanical properties and wettability [20].

A premium class of composite materials known as fibre-reinforced polymer nanocomposites (FRPNCs) incorporates flexible fibres into a polymer matrix that is further strengthened by nanoscale fillers or nanoparticles. Compared to traditional fibre-reinforced polymer composites, the combination of both macroscopic (fibres) and nanoscale (nanoparticle) reinforcement allows for a noticeable enhancement in mechanical, thermal, and barrier properties [21]. Beemkumar et al. developed HC consisting of basalt/Kevlar fibre reinforced with bran filler particulates. The results indicated that the inclusion of bran filler improved thermal and flame-retardant properties due to the synergistic effects of Kevlar and basalt fibres, as well as the char-forming properties of the bran fillers [22]. Turaka et al. (2021) examined the effect of adding MWCNTs and graphene nanoparticles in glass fibre polymer composites with distinct wt% of (0.1–0.3) nanoparticles. The study demonstrated that the glass fibre/epoxy composite, when mixed with 0.2 wt% MWCNTs/graphene, exhibited a 56 % increase in fatigue life, a 36 % enhancement in TS, and a 92.7 % improvement in energy absorption capacity in notched types, compared to the pure composite [23]. Kamatchi et al. (2023) developed coir-based composites with varying weight percentages of graphene nanoparticles (2.5, 5, and 7.5 %). The study revealed that 5 wt% graphene-reinforced coir composites demonstrated higher TS (59 MPa), flexural strength (236 MPa), and impact properties (37 kJ/m<sup>2</sup>) [24]. Reddivari et al. (2024) prepared composites made from jute (jute + cotton)/glass fibre HC with multi-walled carbon nanotubes (MWCNTs) and graphene nanoplatelets (GNPs) at various wt% (0, 0.25, and 0.5) using the vacuum bagging method. Results showed that the 0.25 % MWCNT-GNPs exhibited better mechanical properties compared to other combinations [25]. Lal et al. observed the functional properties of Timoho/epoxy composites with different wt% of graphene filler (2, 3, and 4) using compression moulding. Experimental findings indicated that the composites with 2 wt% graphene exhibited superior tensile, flexural, impact, and interlaminar shear strength [26]. Ganapathy et al. analysed flax/aerial root banyan fibre composites with the inclusion of graphene particles (2, 4, 6, 8 wt%) using compression moulding. The results demonstrated that an HC with 2 % graphene played an essential role in improving the strength of the composite [27]. Kamesh et al. (2024) fabricated composites using glass/sisal fibre with varying amounts of graphene nanoplatelets (GNP) (0 %, 0.25 %, 0.5 %, 0.75 %, and 1 %) in the epoxy matrix. The results suggested that 1.0 wt% GNP in the sisal/glass fibre HC increased TS by 49.7 % and Young's modulus by 60 %. Similarly, flexural strength increased by 228 % and flexural modulus by 362 % compared to sisal/glass HC [28]. Amer et al. studied the impact of adding graphene (0 %, 0.5 %, 1.0 %, and 1.5 %) in flax fibre-reinforced epoxy composites. The optimum

value of 0.5 % graphene nanoparticles enhanced flexural and interlaminar shear strength by 77.7 % and 75.5 %, respectively, compared to other combinations [29]. Dhilipkumar et al. examined the effect of adding graphene to areca/ramie HC. The experimental results concluded that 1.5 wt% graphene increased TS, flexural strength, and impact energy by 187.88 %, 143.17 %, and 159.66 %, respectively [30]. Neuba et al. developed epoxy composites reinforced with sedge fibres (*Cyperus malaccensis*) with the addition of graphene oxide (GO). Results exhibited that incorporating GO into the epoxy matrix significantly improved mechanical properties compared to neat composites [31]. Azka et al. (2025) fabricated composites from bamboo/kenaf reinforced polylactic acid, incorporating graphene nanoplatelets. The findings revealed that GNP-dispersed composites exhibited enhanced mechanical performance compared to pristine samples, and the addition of GNPs also reduced water absorption, as GNPs act as a water barrier within the composite structure [32]. Lubomír et al. fabricated epoxy nanocomposites reinforced with GNPs and halloysite nanotubes (HNTs). The results showed that GNPs incorporation significantly increased ductility, with elongation at break improving by 39 %, while HNTs led to a 20 % reduction in Young's modulus [33].

Although numerous studies have explored using NFs hybridisation to enhance the mechanical properties of polymer composites, the unique combination of ramie and abaca fibres reinforced with GNPs has yet to be investigated, particularly in terms of mechanical and vibrational performance. Unlike previous studies that typically focus on single NFs or various nanofillers, this research highlights the combined effect of hybridising ramie and abaca fibres due to their strength and toughness, alongside GNPs, which are known to improve interfacial bonding and load transfer. The primary aim of this work is to systematically evaluate the impact of this hybridisation on various properties, including TS, flexural

strength, micro-hardness, water absorption, and free vibration characteristics such as natural frequency and damping behaviour, in line with ASTM standards. Additionally, microstructural analysis of tested specimens using FESEM and AFM will provide insight into the interfacial mechanisms that led to enhanced performance. This study fills a crucial gap in the literature by demonstrating how this specific combination of NFs and nanofillers can effectively improve both the static mechanical and vibration properties of ramie/abaca HC.

## 2 Experimental details

### 2.1 Materials

Ramie fibre and abaca fibre were procured from the Fibre Source in Chennai, India. Epoxy LY556 and Hardener HY951 were also obtained from the same supplier. The graphene used in this research had a purity of 99 %, an average thickness of 2.5 nm, a length of 7.5  $\mu\text{m}$ , a bulk density of 0.48 g/cm<sup>3</sup>, and a surface area of 220 m<sup>2</sup>/g. The graphene nanoparticles were sourced from Shilpa Enterprises in Nagpur, Maharashtra, India.

### 2.2 Alkali treatment of ramie and abaca fibre

Initially, we cut the long fibres of ramie and abaca into short fibres, each measuring between 5 mm and 25 mm in length. The short fibres were then cleaned with distilled water to remove dirt and foreign particles. Next, the fibres were immersed in a 5 wt% NaOH solution for 2 h, followed by washing with running tap water for 10–15 min to remove residual NaOH from the fibre surface. Finally, the alkali-treated fibres were dried in an oven at 70 °C for 24 h (Figure 1).

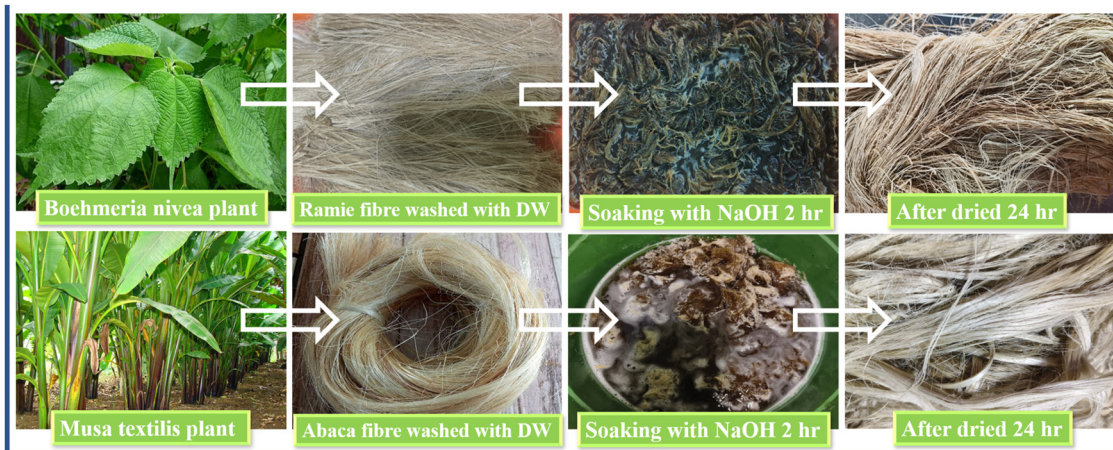


Figure 1: Alkaline treatment of ramie/abaca fibres.

A 5 wt% NaOH solution was chosen based on literature evidence showing it effectively removes hemicellulose, lignin, waxes, and other amorphous components while preserving the crystalline cellulose structure of natural fibres, which is crucial for maintaining their mechanical properties [34–36]. The 2-h treatment time was selected to ensure sufficient removal of surface impurities while minimising fibre damage. Jayabal et al. reported that alkali treatment of coir fibre in epoxy composites using a 5 % NaOH solution resulted in a 31 % increase in TS compared to lower (2 %) and higher (8 %) concentrations [36].

Alkali treatment enhances the surface chemistry of NFs by reducing lignin and waxy substances that act as barriers, thereby exposing more cellulose content. This increases surface roughness and crystallinity, improving mechanical interlocking and chemical compatibility with the epoxy matrix. The drying regime at 70 °C for 24 h was adopted to remove moisture, ensuring stable and consistent fibre properties for composite fabrication.

### 2.3 Synthesis of graphene-modified epoxy resin

Initially, acetone was added to varying weight percentages of graphene particles (0.5, 1.0, 1.5, and 2.0) in the beaker. We used an ultrasonication technique, with a power of 70 W, to mix the acetone and graphene at 40 kHz for 30 min. Next, we added the required quantity of epoxy to the acetone-graphene mixture. The resulting mixture was magnetically stirred at 80 °C to remove the acetone, and the precise

amounts of epoxy, graphene, and acetone were carefully measured and controlled to ensure complete solvent evaporation and prevent residual solvent from affecting the curing process. It was then kept in a vacuum oven at 0.25 bar pressure for 30 min at 28 °C to eliminate air pockets and any remaining traces of solvent. The resulting graphene-epoxy-modified blend was then mixed with hardener HY951 in a 10:1 resin-to-hardener ratio (Figure 2). This process ensured strong interfacial bonding and uniform dispersion of graphene, which was affirmed using AFM.

### 2.4 Ramie/abaca/epoxy HC preparation

The treated short fibres of ramie (15 wt%) and abaca (15 wt%) with various wt% of (0.5, 1.0, 1.5, and 2.0) graphene-reinforced epoxy HC were prepared using the compression moulding method. Initially, the required quantity of a graphene-modified epoxy mixture (70 wt%) was poured over the randomly oriented ramie-abaca short fibre in the steel mould, as illustrated in Figure 3. The excess resin is removed by rotating the roller over the fibre's surface. The top and bottom plates of the mould are enclosed by a steel plate and placed over the compression moulding machine at 35 kg/cm<sup>2</sup> pressure and a temperature of 50 °C for a duration of 24 h. The hybrid composites were initially fabricated into plates with fixed dimensions of 300 × 300 × 5 mm using the compression moulding process. Afterwards, the test specimens were carefully sliced according to the relevant ASTM standard dimensions. The composition of the ramie/abaca HC is illustrated in Table 1.

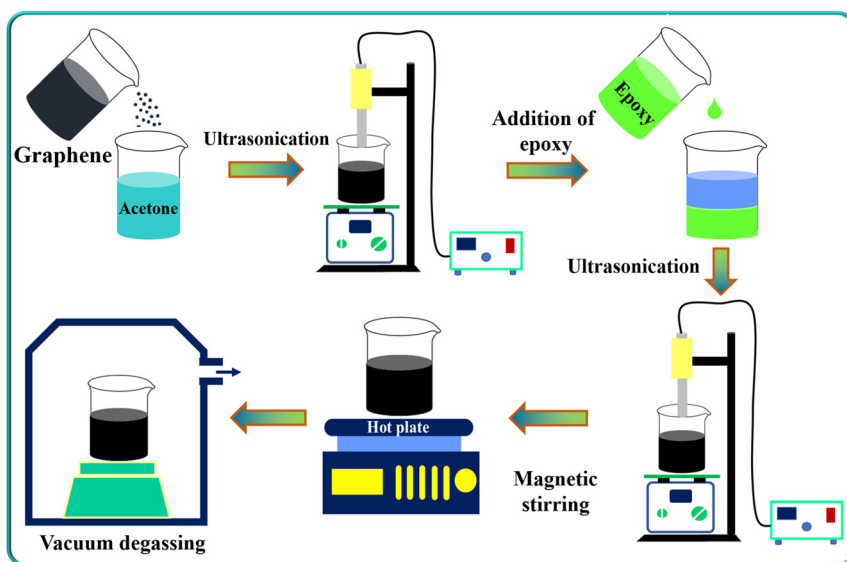


Figure 2: Preparation of graphene/epoxy mixture.



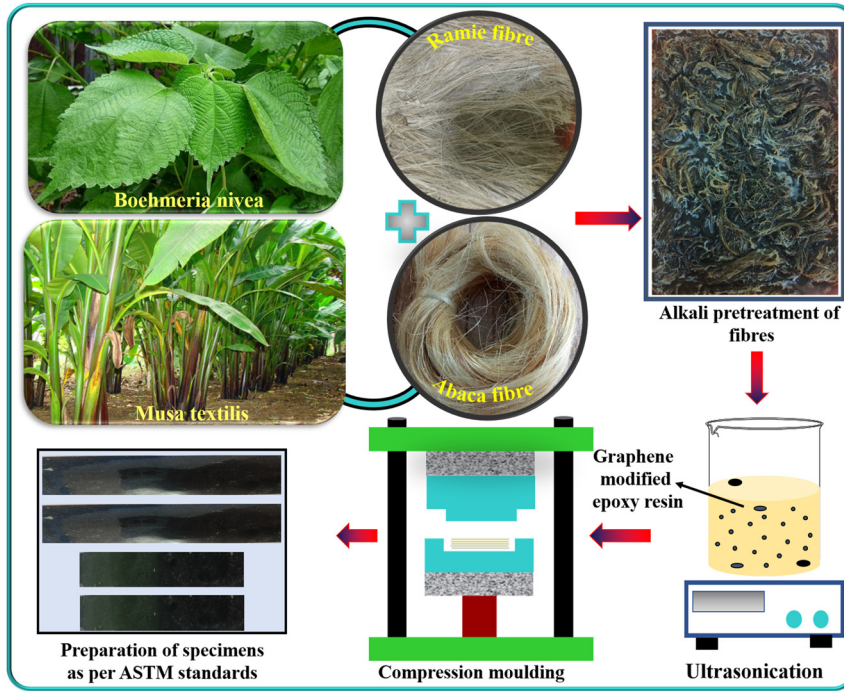


Figure 3: Preparation of ramie/abaca HC.

Table 1: Composition of ramie/abaca fibre reinforced epoxy composites.

Sl. No	Sample name	Epoxy resin wt%	Ramie fibre wt%	Abaca fibre wt%	Graphene wt%	Theoretical density (g/cm <sup>3</sup> )	Experimental density (g/cm <sup>3</sup> )
1	RA0.0	70	15	15	0	1.14	1.11
2	RA0.5	70	14.75	14.75	0.5	1.08	1.13
3	RA1.0	70	14.5	14.5	1.0	1.12	1.10
4	RA1.5	70	14.25	14.25	1.5	1.16	1.14
5	RA2.0	70	14	14	2.0	1.10	1.14

## 2.5 Density measurement

The theoretical density of the composites, based on the weight fractions of the different constituents, can be calculated using the following Eq. (1).

$$\rho_{ct} = 1 / \left[ (w_{fa} / \rho_{fa}) + (w_{fr} / \rho_{fr}) + (w_m / \rho_m) \right] \quad (1)$$

Where  $\rho_{ct}$  = theoretical density of the composite,  $\rho_{fa}$  = density of abaca fibre,  $\rho_{fr}$  = density of ramie fibre,  $\rho_m$  = density of epoxy matrix,  $w_{fa}$ ,  $w_{fr}$ , and  $w_m$  = weight fractions of abaca fibre, ramie fibre, and matrix, respectively. The experimental density of the composites was determined using the water immersion method based on Archimedes' principle, in accordance with ASTM D 570–98 (Table 1).

## 3 Material characterisation

### 3.1 Tensile, flexural and impact testing

Ramie/abaca HC were tested to determine their tensile and flexural properties. Tensile properties were assessed by using an Instron 8801 universal testing machine (UTM), and flexural properties were evaluated using the Tinius Olsen UTM, as shown in Figure 4(a and b). For evaluating TS, a 2 mm/min strain rate and a 50 kN load cell were used. The tensile specimens were made with dimensions of 250 mm, 25 mm, and 5 mm, as per the ASTM D 3039 standard. The specimens utilised in the flexural test had the following dimensions: 127 mm by 25 mm by 5 mm (ASTM D790), a strain

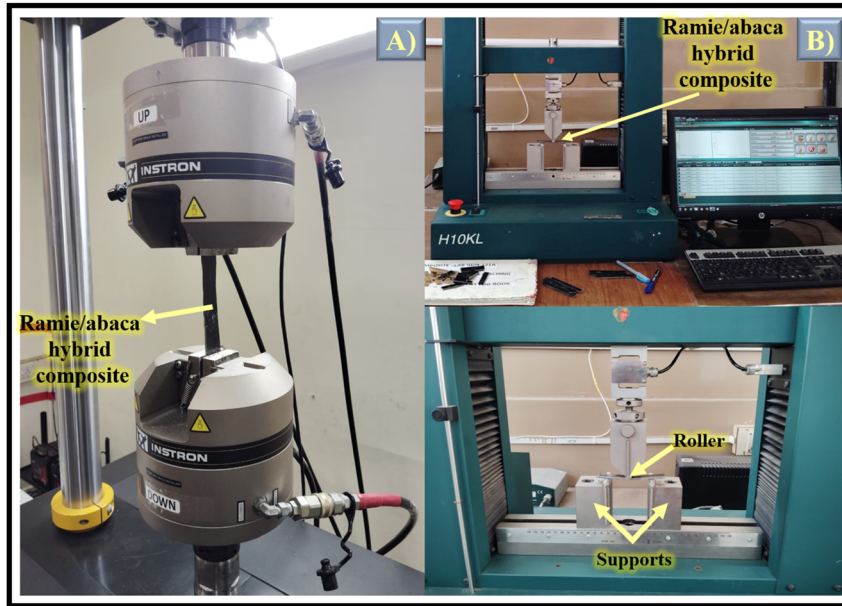


**Figure 4:** Mechanical testing of ramie/abaca fibre-reinforced HC (a) tensile analysis, (b) flexural test.

rate of 2 mm/min, and a 10 kN load cell. For each experiment, three samples were chosen to assess the composite's tensile and flexural strengths. Impact test was carried out according to the ASTM D256. For that, the samples were fixed vertically, and a 5 kg pendulum with a 150° folding angle and 2.5 m/s velocity was used for impact loading.

### 3.2 Free vibration analysis

For carrying out free vibrational analysis, the ramie/abaca HC is stimulated using the impulse hammer method (Figure 5). The samples were excited using a Dytran impulse hammer, and a lightweight sensor was utilised to record the vibration response. The DEWE four-channel data-collecting system provides the force input and vibration response, which vary over time, to the DEWE 7 modal analysis software. The software then transforms the time-domain data into a frequency-domain signal using Fast Fourier Transformation (FFT). The frequency response function is produced by evaluating the reactions to impulse excitations at different selected locations. The NF, modal damping ratio, and free vibration mode for a particular mode are then immediately provided by the software. The modal damping of a given mode is determined using the circle fit method, which involves a specific relationship (Equation (2)).

$$\varepsilon = \frac{\omega_2^2 - \omega_1^2}{2\omega_0 \left[ \omega_2 \tan \frac{\alpha_2}{2} + \omega_1 \tan \frac{\alpha_1}{2} \right]} \quad (2)$$

The angular frequency at resonance is represented as  $\omega_0$ , where  $\omega_1$  &  $\omega_2$  denote angular frequencies  $\alpha_1$  &  $\alpha_2$  are the angles between the angular frequencies.

### 3.3 Micro-hardness

Using a Shore D hardness tester (Model: MGW Precision Tools), the hardness of the developed ramie/abaca HC was assessed following ASTM D2240-15 testing guidelines. This test measures the hardness of rubbers, elastomers, polymers, and plastics. Ten different areas were evaluated for hardness, and the average value was determined. A material is considered highly resilient if its digital value exceeds 60. Values under 60 suggest that the material is not very resilient.

### 3.4 Water absorption and contact angle analysis

Ramie/abaca HC samples with dimensions of 64 mm × 12.7 mm × 5 mm were used for the water absorption test, as per ASTM D570–98 guidelines. The samples were placed in a desiccator and dried for one day at 60 °C before being allowed to cool to ambient temperature. The initial weight of the specimen was then measured ( $W_i$ ). After that, the samples were immersed in deionised water at ambient temperature. The composites were removed from the water every one day, wiped with a cotton cloth to remove water from the composite surface, weighed again ( $W_f$ ), and then returned to the water. For 15 days, this method was repeated. The following Eq. (3) was utilised to determine the amount of water absorbed by the specimens.  $\mu$ .

$$\%W = \frac{W_f - W_i}{W_i} \times 100 \quad (3)$$

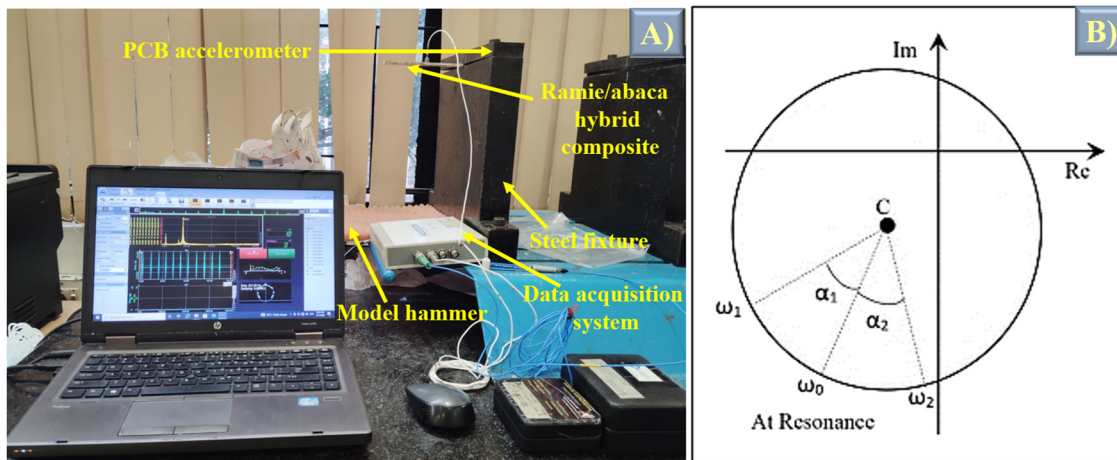


Figure 5: Free vibrational analysis of graphene-reinforced ramie/abaca HC.

The contact angle analysis was conducted using a goniometer, specifically the Kyowa contact angle meter (DME-211 series). The water droplet size ( $4\ \mu\text{L}$ ) and capture time (40 s) remained unchanged for all composites, following the release of a droplet onto a  $2\text{ cm} \times 2\text{ cm}$  sample area. For each configuration, three samples were assessed, and the average contact angle values along with their corresponding standard deviations were recorded.

### 3.5 Microstructure analysis

FE-SEM, Carl Zeiss- Sigma 300, was used to analyse the fractured HC samples, which had dimensions of  $10\text{ mm} \times 10\text{ mm} \times 5\text{ mm}$ , at an acceleration voltage of 20 kV. Gold coating was applied to the samples using a sputter coating process to improve conductivity. AFM, Model: Nanosurf AFM was used to analyse the dispersion of graphene particles in the prepared composite.

## 4 Results and discussion

### 4.1 Tensile behaviour of ramie/abaca HC

Figure 6(a–d) depicts the tensile behaviour of ramie/abaca HC prepared with distinct wt% of graphene. The tensile analysis (Table 2) shows that the addition of graphene improves the TS of composites compared to neat composites.

The tensile properties increased with up to 1.5 wt% graphene inclusion; however, further additions resulted in lower tensile properties compared to the presence of 1.0 and 1.5 wt% graphene. The sample reinforced with 1.5 wt% graphene exhibited a TS of 22 MPa and a modulus of

3,116.897 MPa, which are 175 % and 93.77 % higher than those of neat composites. This indicates that adding graphene to epoxy enhances its ability to bear more load and provides higher resistance to tensile loading. This improvement is a result of the nanoscale reinforcement effect of well-dispersed graphene, which strengthens interfacial adhesion and stress transfer between the matrix and NFs. Meanwhile, the inclusion of 2.0 wt% graphene demonstrated lower TS (17 MPa) and modulus (2,835.162 MPa) compared to samples prepared with 1.5 wt% graphene. This decline is primarily caused by the agglomeration of excess graphene at elevated filler contents, which acts as stress intensification sites and disrupts the matrix's continuity, thereby weakening the composite. The reason for the improvement in TS is the even distribution of graphene in the epoxy matrix, which facilitates better bonding between NFs, as confirmed by AFM (Figure 7).

Moreover, examining tensile-tested samples using FESEM has revealed that the inclusion of graphene influences the microstructure of the ramie/abaca HC. The damage to the matrix and fibres, along with poor bonding between them, is evident in Figure 8(a), which is the reason for the lower load-carrying capacity of the neat composites. However, with a 1.5 wt% loading of graphene, the presence of nanoparticles helps carry more load owing to better adhesion between the matrix and NFs, as shown in Figure 8(b). The samples with higher graphene content failed at a lower load compared to those with 1.5 wt% loading, due to the accumulation (Figure 8(c)) of nanoparticles in the matrix, which decreased the load-carrying ability and caused early failure from matrix and fibre damage, as shown in Figure 8(d).

The TS of ramie/abaca HC was improved by 62.5 %, 137.5 %, 175 %, and 112.5 %, respectively, compared to unmodified composites. A similar kind of observation was also

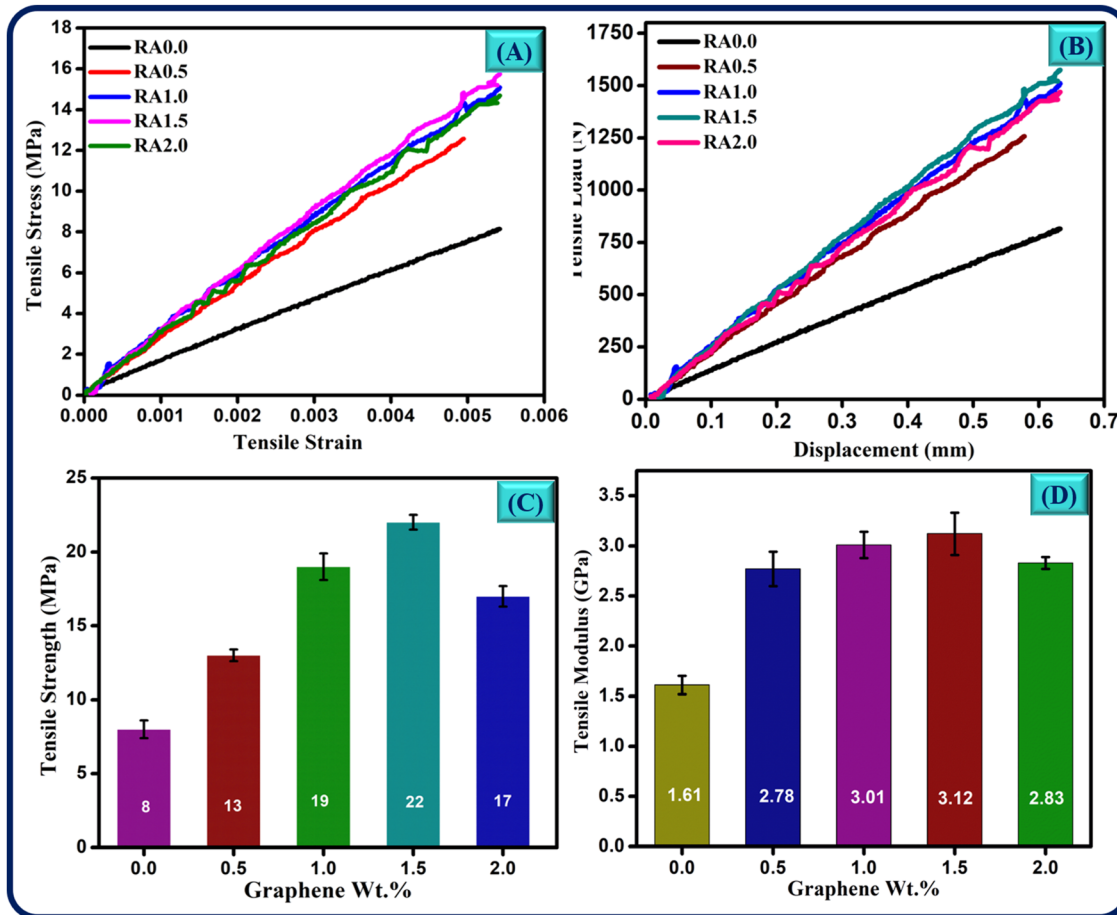


**Figure 6:** Tensile behaviour of ramie/abaca HC (a) load versus displacement, (b) stress versus strain, (c) tensile strength versus graphene wt%, (d) tensile modulus versus graphene wt%.

**Table 2:** Tensile behaviour of ramie/abaca HC.

Sl. No	Sample code	Graphene wt%	Tensile strength (MPa)	% Increment tensile strength	Modulus (MPa)	% Increment modulus
1	RA0.0	0.0	8 ± 0.82	–	1,608.546	–
2	RA0.5	0.5	13 ± 1.03	62.5	2,773.013	72.39
3	RA1.0	1.0	19 ± 0.91	137.5	3,013.414	87.33
4	RA1.5	1.5	22 ± 0.44	175	3,116.897	93.77
5	RA2.0	2.0	17 ± 1.26	112.5	2,835.162	76.25

noted by researchers; for instance, Hosseini et al. found that incorporating 2 wt% graphene to glass fibre/NFs has enhanced the TS by 37 % [37]. Dhilipkumar et al. also stated that adding graphene has improved the TS of kenaf/pine-apple fibre composite by 133.75 %. The present study confirmed that the incorporation of graphene significantly enhances the tensile strength of HC, highlighting its potential as an effective reinforcement in weight-sensitive structural applications [38].

## 4.2 Flexural properties of ramie/abaca HC

The flexural behaviour of ramie/abaca HC infused with graphene nanopowder is illustrated in Figure 9(a–c). A transverse bending load was applied to assess the failure loads of the HC. The flexural results indicated that the addition of graphene improved the flexural strength of the composites compared to neat composites (Table 3). Findings show that ramie/abaca HC prepared with 1.5 wt% graphene



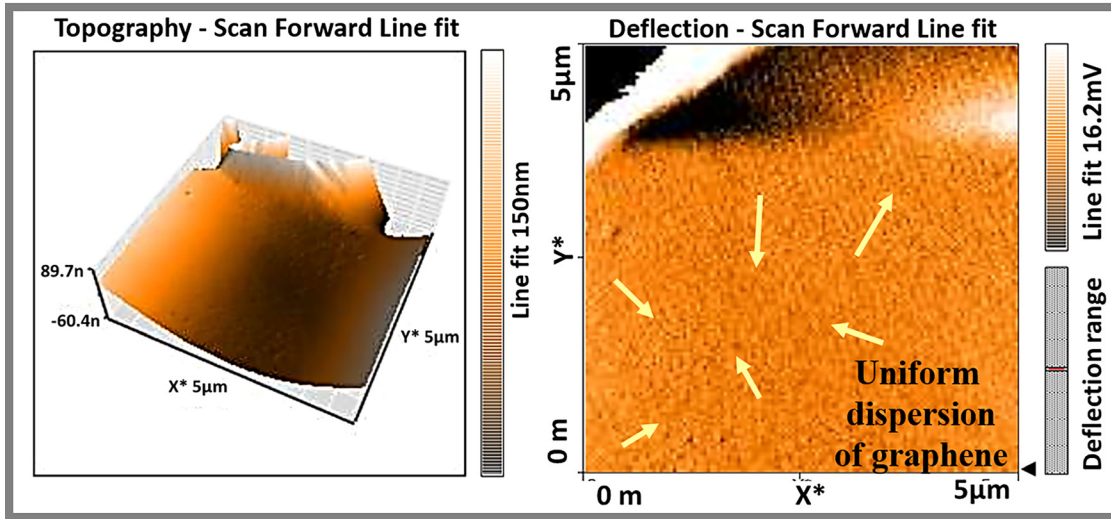


Figure 7: Uniform dispersion of graphene 1.5 wt% in epoxy matrix.

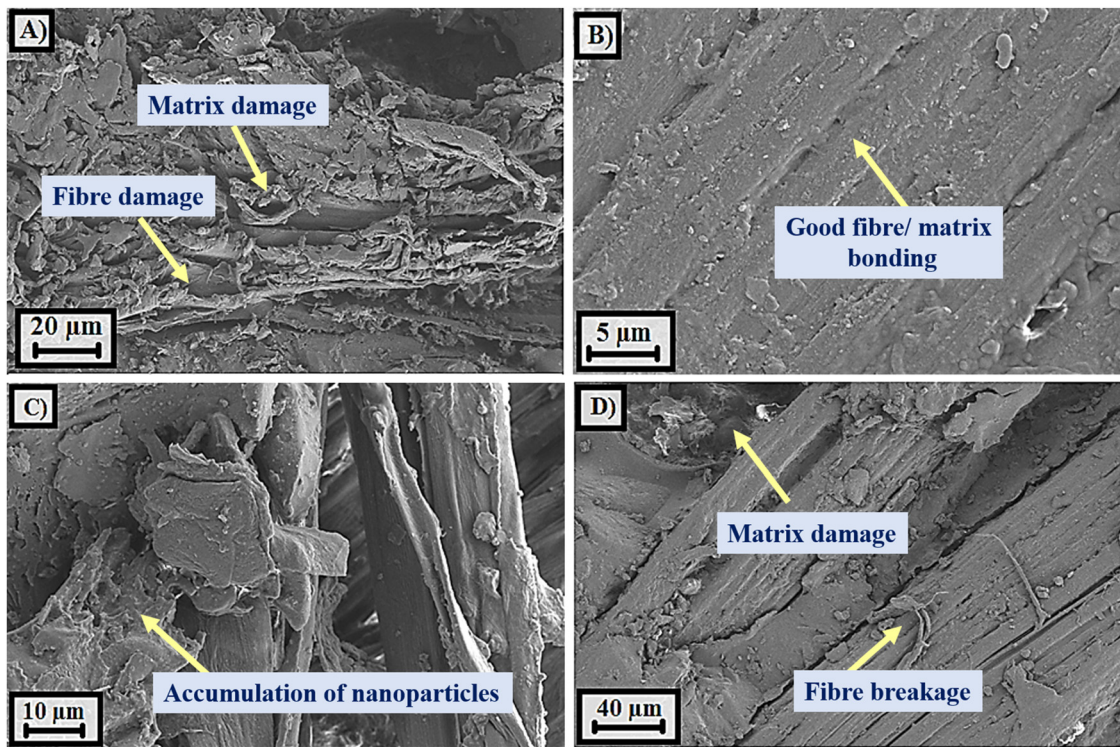


Figure 8: FESEM image of ramie/abaca HC (a) neat composite, (b) 1.5 wt%, (c) 2.0 wt%, (d) 2.0 wt%.

enhanced the flexural strength of the composites compared to neat composites. This improvement can be ascribed to the more efficient distribution of stress and the crack-bridging ability of the well-dispersed graphene, which reinforces the epoxy matrix and strengthens the fibre-matrix surface. The inclusion of graphene in the matrix reduced fibre pull-out and matrix damage, enabling it to support higher loads than

other composites. Meanwhile, the sample containing 2.0 wt% graphene exhibited a lower flexural strength of 61.47 MPa compared to the samples with 1.5 wt% graphene (70.64 MPa) due to the slight accumulation of graphene in the epoxy matrix. Such agglomeration acts as micro-defects that initiate premature cracking under flexural loads, thereby lowering the overall strength.

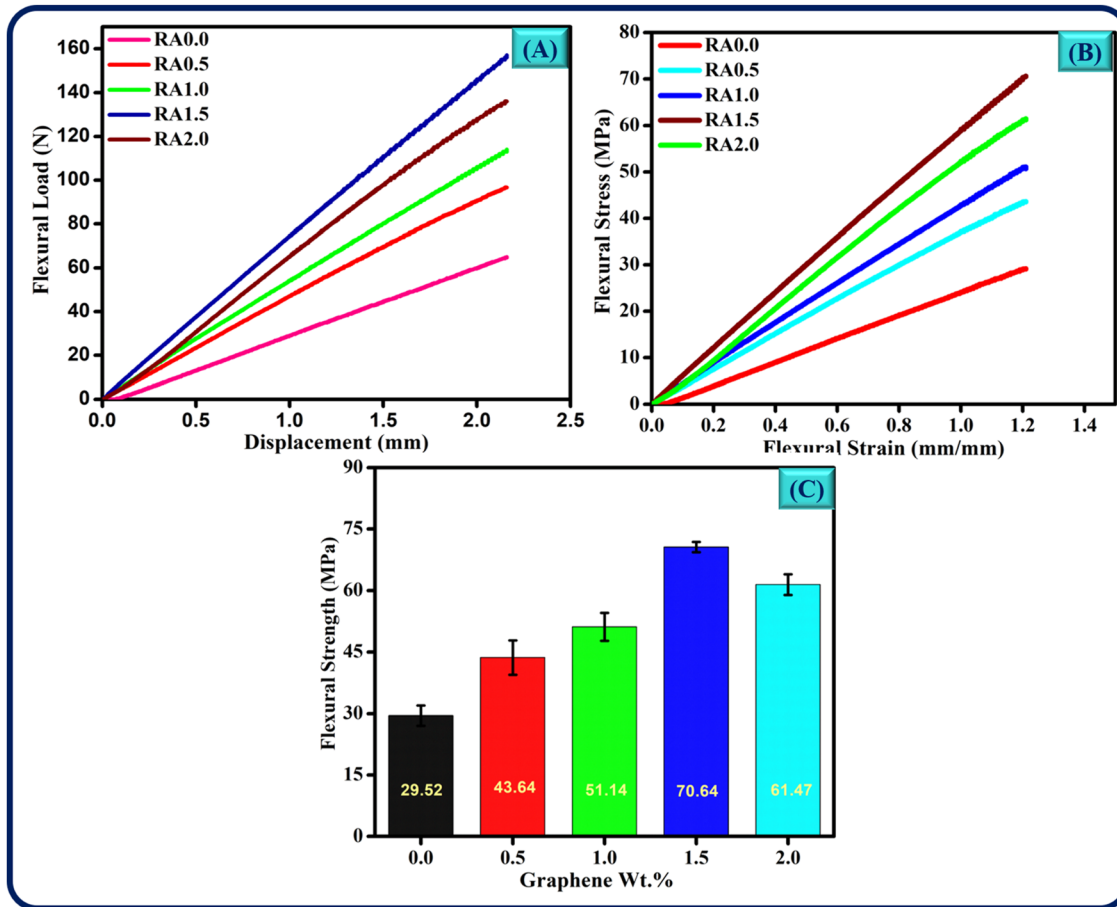


Figure 9: Flexural behaviour of ramie/abaca HC (a) load versus displacement, (b) stress versus strain, (c) flexural strength versus graphene wt%.

Table 3: Flexural behaviour of ramie/abaca HC.

Sl. No	Sample code	Graphene wt%	Flexural strength (MPa)	% increment
1	RA0.0	0.0	29.52 ± 2.85	–
2	RA0.5	0.5	43.64 ± 4.20	47.83
3	RA1.0	1.0	51.14 ± 3.80	73.23
4	RA1.5	1.5	70.64 ± 1.25	139.29
5	RA2.0	2.0	61.47 ± 2.54	108.23

The examination of tensile test samples using FESEM has revealed that the incorporation of graphene has influenced the microstructure of the ramie/abaca HC. As shown in Figure 10(a), adding 1.5 wt% graphene has aided in better bonding between fibre and matrix, with resin-rich regions providing more resistance to transverse loading. The well-bonded interface facilitates effective load transfer, delays crack propagation, and enhances energy absorption during flexural deformation. Meanwhile, increasing the concentration leads to lower resistance to transverse loading because matrix accumulation reduces interfacial adhesion,

which in turn prompts significant matrix and fibre damage, as evident from Figure 10(b–d).

The flexural strength of ramie/abaca HC was improved by 47.83 %, 73.23 %, 139.29 %, and 108.23 %, respectively, compared to unmodified composites. Researchers also noted a similar observation; for instance, Sasikumar et al. also reported that adding graphene to caesar weed fibre and roselle fibre HC has enhanced flexural properties owing to better bonding between the fibre and matrix [39]. Ashok et al. fabricated and inspected the luffa/Kevlar fibre composite reinforced with graphene. Results have shown that the accumulation of graphene improved the flexural strength by 25.2 % compared to neat composites [40].

### 4.3 Impact properties of ramie/abaca HC

Figure 11 illustrates the impact behaviour of HC under impact loading according to ASTM D 256 standards. The addition of graphene significantly enhanced the energy-absorbing capacity of the composites compared to the pure



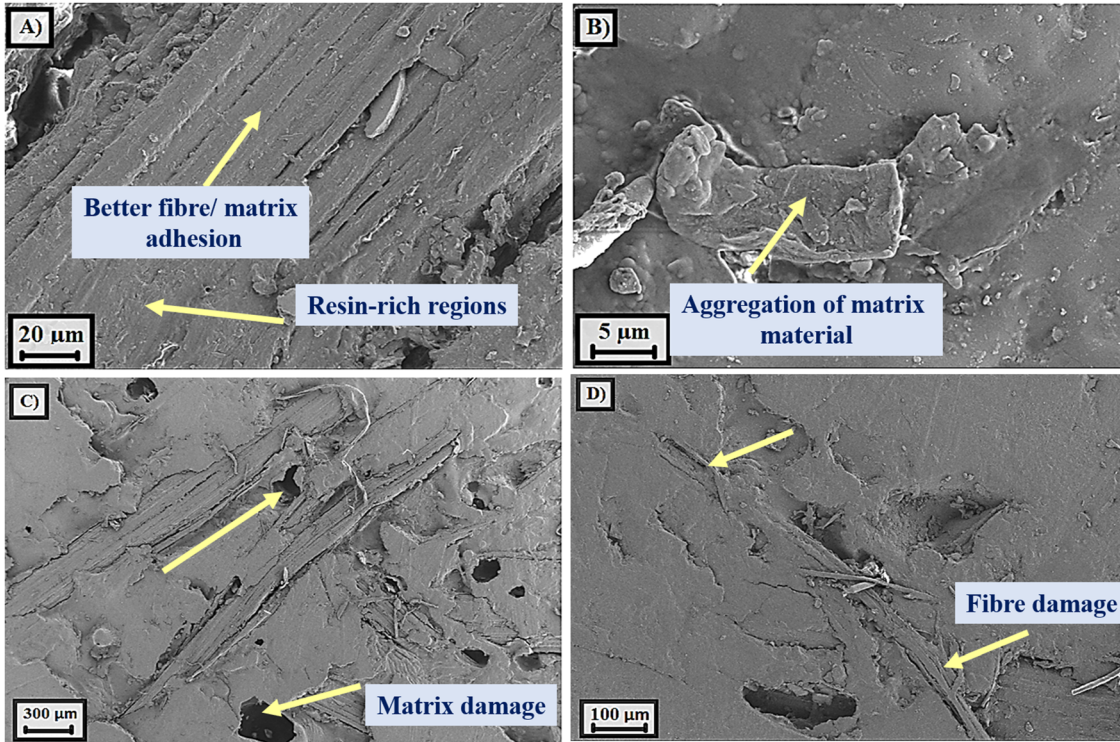


Figure 10: FESEM image of ramie/abaca HC (a) 1.5 wt%, (b) 2.0 wt%, (c) 2.0 wt%, (d) 2.0 wt%.

HC (RA0.0), which had an impact strength of 2.41 J. When 0.5 wt% graphene was added (RA0.5), the impact strength increased to 3.58 J, a 48.54 % rise. Increasing the graphene content to 1.0 wt% (RA1.0) resulted in an impact strength of 4.69 J, a 94.60 % improvement over the neat composite. The highest increase was observed at 1.5 wt% graphene (RA1.5), where the impact strength reached 5.94 J, a 146.47 % increase.

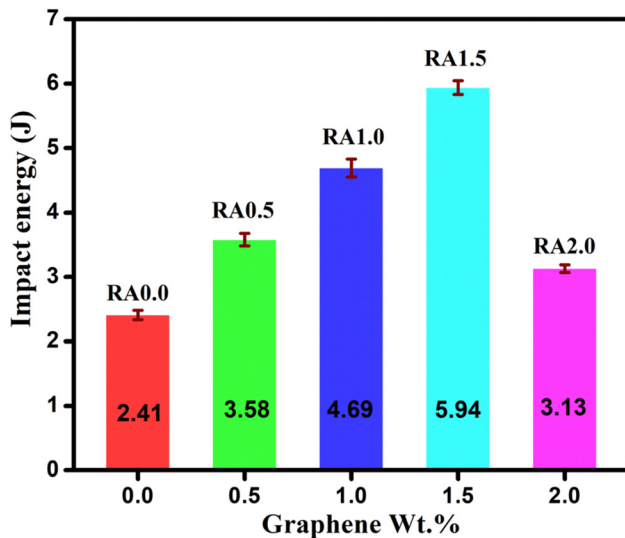


Figure 11: Impact behaviour of ramie/abaca HC.

This notable enhancement is due to better interfacial bonding between the ramie/abaca fibres and the epoxy matrix, facilitated by well-dispersed GNPs, which improved stress transfer and energy dissipation during impact loading. However, at 2.0 wt% graphene (RA2.0), the impact strength decreased to 3.13 J, showing only a 29.87 % increase compared to the neat composite. This decline is caused by graphene agglomeration at higher concentrations, which weakens interfacial bonding and promotes crack growth under impact. These findings emphasise that an optimal graphene content (1.5 wt%) is crucial for maximising impact performance, while excessive loading results in lower impact resistance.

#### 4.4 Free vibrational behaviour of ramie/abaca HC

The free vibration properties of areca/ramie HC with varying graphene content were evaluated under fixed-free boundary conditions using an impulse hammer technique. The results demonstrated that the existence of graphene significantly influenced both the NF and the damping behaviour of the composites for the three mode shapes (Figure 12(a–c)).

The unmodified sample (RA0.0) without graphene exhibited NF of 45.775 Hz, 270.94 Hz, and 784.5 Hz for modes

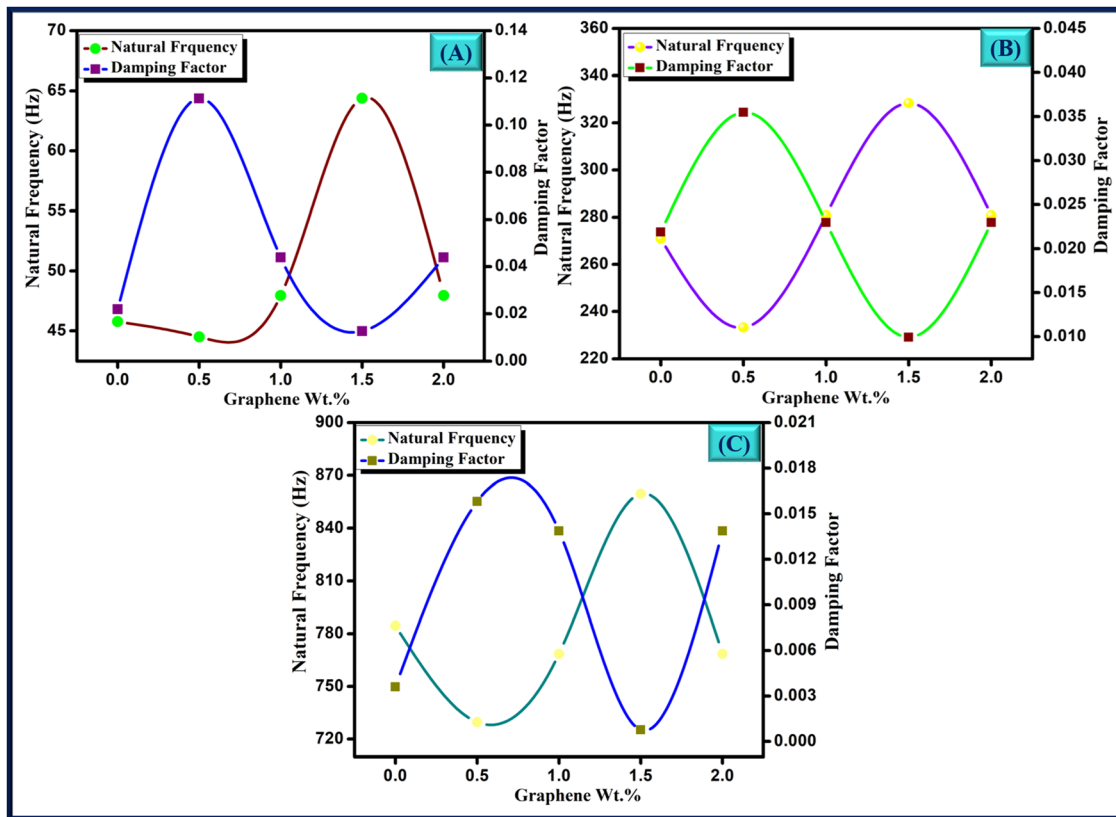


Figure 12: Free vibrational behaviour of ramie/abaca HC (a) mode 1, (b) mode 2, (c) mode 3.

1, 2, and 3, respectively, with damping factors of 0.021945, 0.021887, and 0.0036083. With the introduction of 0.5 wt% graphene (RA0.5), there was a slight reduction in NF, while damping factors increased to 0.11134, 0.035496, and 0.015821, respectively, possibly due to changes in interfacial bonding. As the graphene content increased to 1.0 wt% (RA1.0), the NF improved to 47.952 Hz, 280.78 Hz, and 768.59 Hz, with moderately lower damping values, indicating that the presence of graphene enhanced the stiffness and reduced energy dissipation to some extent. The most significant improvement was observed at 1.5 wt% graphene (RA1.5), where the composite achieved the highest NF of 64.39 Hz, 328.41 Hz, and 859.6 Hz, along with the lowest damping values of 0.012628, 0.0099287, and 0.00076811. This indicates that the presence of graphene at this concentration greatly improved the fibre-matrix interaction and stiffness of the composite. However, a further increase in graphene content to 2.0 wt% (RA2.0) did not yield additional benefits; the NF dropped back to values similar to the 1.0 wt% sample, and damping increased again. This may be ascribed to the potential agglomeration of graphene at higher concentrations, which could reduce interfacial efficiency. In summary, 1.5 wt% graphene was found to be the most effective concentration for increasing the vibrational enactment of areca/ramie HC.

#### 4.5 Shore D hardness

The Shore D hardness of ramie/abaca HC was assessed with varying graphene content ranging from 0 to 2.0 wt%, and the results are shown in Figure 13. The neat composite without graphene exhibited an average hardness value of 76, which increased progressively with the inclusion of graphene. At 0.5 wt% graphene, the hardness improved to 78.8, and further increased to 80.8 at 1.0 wt%. The highest Shore D hardness was observed for the composite with 1.5 wt% graphene, reaching an average value of 82.2, as shown in Figure 13. This significant enhancement can be attributed to the presence of graphene, which reinforces the polymer matrix and restricts localised deformation, thereby increasing surface resistance to indentation. However, at 2.0 wt% graphene, a slight reduction in hardness was noted (79.2), possibly due to graphene agglomeration, which may have led to stress concentration points and uneven distribution, thereby affecting the material's surface integrity. Overall, the results suggest that incorporating graphene up to 1.5 wt% significantly enhances the surface hardness of ramie/abaca HC, while higher concentrations may lead to a reduction in hardness due to potential graphene agglomeration and compromised filler dispersion.



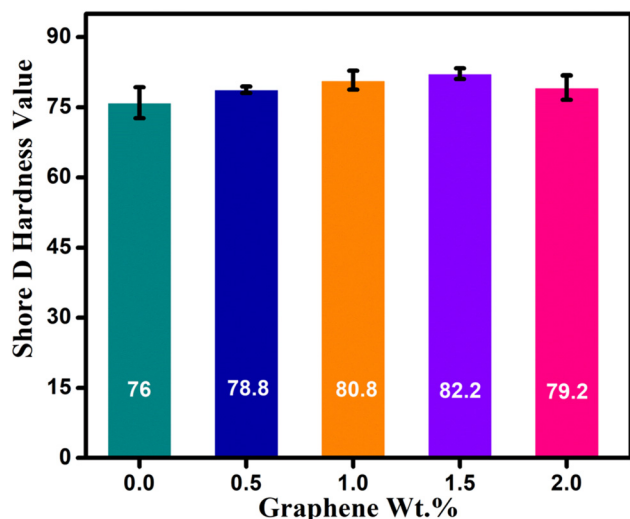


Figure 13: Shore D hardness of ramie/abaca HC.

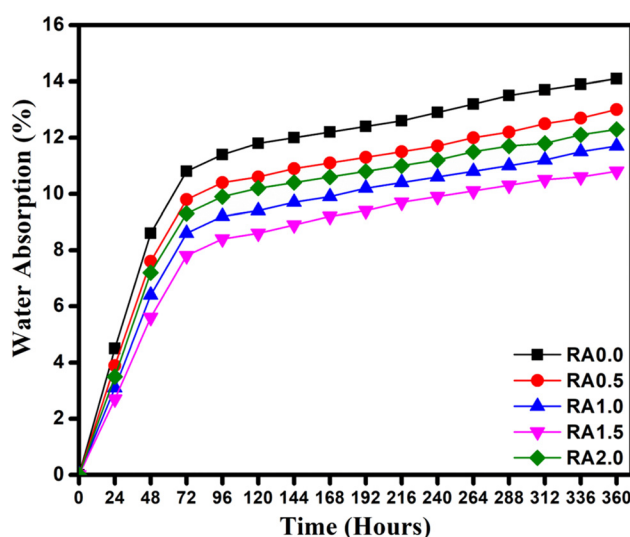


Figure 14: Water absorption behaviour of ramie/abaca HC.

#### 4.6 Wettability analysis of ramie/abaca HC

Figure 14 depicts the water absorption performance of ramie/abaca fibre-reinforced epoxy composites with varying graphene content (0–2.0 wt%). NFs like ramie and abaca have hydroxyl-rich cellulose structures that easily form hydrogen bonds with water molecules, making them naturally hydrophilic. When used as reinforcements in polymer composites, their ability to absorb moisture can limit the long-term performance of these materials. However, hybridisation and the use of nanofillers, such as graphene, can help mitigate this behaviour by improving the fibre-matrix interface and reducing water diffusion pathways.

Across all tested samples, the composites demonstrated a typical two-stage water absorption pattern: an initial rapid intake followed by gradual stabilisation as saturation approached. The neat ramie/abaca composite without graphene had the highest water uptake, reaching 14.1 %, owing to the NFs high moisture affinity. The addition of 0.5 wt% graphene reduced water absorption to 13.0 %, indicating improved interfacial adhesion that limited capillary voids and micro-channels in the matrix. Further graphene loading to 1.0 wt% and 1.5 wt% resulted in reduced uptake values of 11.7 % and 10.8 %, respectively, which were the lowest recorded in the study. These reductions indicate that the presence of graphene improves the matrix's compactness and effectively acts as a water barrier. However, a slight increase in water absorption was witnessed in the composite containing 2.0 wt% graphene, which had a water uptake of 12.3 %. This marginal increase can be attributed to graphene's tendency to agglomerate at higher concentrations, resulting in microstructural defects and loosely bonded regions that allow moisture to penetrate.

Water contact angle (WCA) measurements supported these findings (Figure 15(a–e)). The ramie/abaca composite had a WCA of 67.2°, indicating its hydrophilic nature. The addition of graphene increased the contact angle in all modified composites, indicating a lower surface affinity for water. Composites with 1.0 wt% and 1.5 wt% graphene had the highest WCAs of 79.3° and 80.7°, respectively. Composites

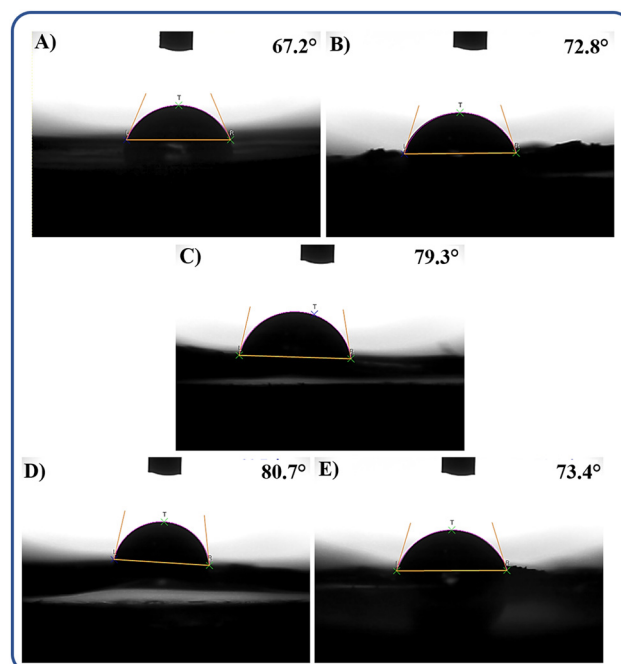


Figure 15: Water contact analysis of ramie/abaca HC (a) neat composites, (b) 0.5 wt%. (c) 1.0 wt% (d) 1.5 wt% (e) 2.0 wt%.

with 1.5 wt% and 2.0 wt% graphene showed improved resistance to wetting in contrast to the unmodified sample. The enhancement in WCA is attributed to graphene's ability to reduce the composite's surface energy and partially shield the fibres from direct contact with moisture. Ganapathy et al. (2024) also found that adding 2.0 wt% graphene has reduced the moisture absorption behaviour of HC made from flax fibre and aerial root banyan fibre [27]. In summary, adding graphene to ramie/abaca HC effectively reduces water absorption and improves surface hydrophobicity, with optimal performance observed at 1.0–1.5 wt% graphene. Beyond this point, the benefits begin to wane due to nanoparticle agglomeration.

## 5 Conclusions

This study thoroughly investigated how the varying concentrations of graphene nanoparticles (0.5, 1.0, 1.5, and 2.0 wt%) affected the mechanical, vibrational, and moisture resistance properties of ramie/abaca HC. The optimal loading was found to be 1.5 wt% graphene, leading to a TS of 22 MPa and a modulus of 3,116.897 MPa, reflecting increases of 175 % and 93.77 %, respectively, over the neat composite. Likewise, the flexural strength reached a peak of 70.64 MPa, representing a 139.29 % improvement over the unmodified sample, attributed to enhanced stress transfer and crack resistance. FESEM and AFM analyses validated improved fibre/matrix adhesion and a uniform distribution of graphene at this concentration. Vibrational analysis revealed that the highest NF and lowest damping ratios were observed at a 1.5 wt% graphene concentration, indicating enhanced dynamic stiffness and energy retention. Surface hardness also increased significantly, achieving a maximum Shore D value of 82.2. Water absorption tests demonstrated a consistent reduction in moisture uptake with rising graphene levels up to 1.5 wt%, decreasing from 14.1 % in the neat composite to 10.8 %. However, beyond 1.5 wt%, performance metrics in all evaluated parameters saw a slight drop due to graphene agglomeration, which caused defects and weakened interfacial interactions. Overall, the results confirm that graphene acts as an effective reinforcing agent for ramie/abaca fibre composites, with 1.5 wt% providing the best enhancements in both structural and functional properties. The developed abaca/ramie HC with graphene filler are suitable for secondary applications in the automotive, marine, and aerospace sectors. They can be used in automotive interior panels, dashboard components, and seat backs; marine cabin panels and storage compartments; and aerospace interior linings and luggage compartments. These applications

leverage the lightweight nature and improved vibration resistance of the composites, where moderate mechanical strength is sufficient.

**Funding information:** This work was supported and funded by the Deanship of Scientific Research at Imam Mohammad Ibn Saud Islamic University (IMSIU) (grant number IMSIU-DDRSP2503).

**Author contributions:** Writing – methodology, investigation, conceptualisation, Writing – original draft, formal analysis, data curation: M.B.B.H, T.D. and S.A.; Conceptualisation, funding acquisition: A.M.S and M.B.B.H; Review & editing: P.K.; Writing–review, Investigation and editing, supervision: K.V.S.; Review and editing: M.R.; Review and editing, data curation: N.A. All authors have accepted responsibility for the entire content of this manuscript and approved its submission.

**Conflict of interest:** The authors state no conflict of interest.

**Data availability statement:** The datasets generated and/or analysed during the current study are available from the corresponding author on reasonable request.

## References

1. Brindha G, Arul SJ, Lenin AH, Premila JSK. Investigation of the effects of water uptake on the mechanical properties of wood dust particle filled Prosopis Juliflora reinforced phenol formaldehyde hybrid polymer composites. *Int Polym Process* 2024;39:125–33.
2. Sepetcioglu H, Lapčík L, Lapčíková B, Vašina M, Hui D, Ovsík M, et al. Improved mechanical properties of graphene-modified basalt fibre–epoxy composites. *Nanotechnol Rev* 2024;13:20240052.
3. Mustafa MA, Tayeh BA, Ahmed TI, Bashir MO, Tobbala DE. Influence of nano-silica and nano-ferrite particles on mechanical and durability of sustainable concrete: a review. *Nanotechnol Rev* 2025;14: 20250151.
4. Skosana SJ, Khoathane C, Malwela T. Driving towards sustainability: a review of natural fiber reinforced polymer composites for eco-friendly automotive light-weighting. *J Thermoplast Compos Mater* 2025;38: 754–80.
5. Jagadeesh P, Puttegowda M, Boonyasopon P, Rangappa SM, Khan A, Siengchin S. Recent developments and challenges in natural fiber composites: a review. *Polym Compos* 2022;43:2545–61.
6. Birniwa AH, Abdullahi SSA, Ali M, Mohammad REA, Jagaba AH, Amran M, et al. Recent trends in treatment and fabrication of plant-based fiber-reinforced epoxy composite: a review. *J Compos Sci* 2023;7: 120–53.
7. Neto J, Queiroz H, Aguiar R, Lima R, Cavalcanti D, Banea MD. A review of recent advances in hybrid natural fiber reinforced polymer composites. *J Renew Mater* 2022;10:561–90.
8. Naik V, Kumar M, Kaup V. A review on natural fiber composite material in automotive applications. *Eng Sci* 2021;18:1–10.
9. Kandasamy J, Soundhar A, Rajesh M, Mallikarjuna Reddy D, Kar VR. Natural fiber composite for structural applications. Structural health monitoring system for synthetic, hybrid and natural fiber composites. *Compos Sci Technol* 2021;6:23–35.

10. Ramesh M, Rajeshkumar LN, Srinivasan N, Kumar DV, Balaji D. Influence of filler material on properties of fiber-reinforced polymer composites: a review. *E-Polymers* 2022;22:898–916.
11. Suriani MJ, Ilyas RA, Zuhri MYM, Khalina A, Sultan MTH, Sapuan SM, et al. Critical review of natural fiber reinforced hybrid composites: processing, properties, applications and cost. *Polymers* 2021;13:3514.
12. Haris NIN, Hassan MZ, Ilyas RA, Suhot MA, Sapuan SM, Dolah R, et al. Dynamic mechanical properties of natural fiber reinforced hybrid polymer composites: a review. *J Mater Res Technol* 2022;19:167–82.
13. Hiremath A, Nayak SY, Heckadka SS, Pramod JJ. Mechanical behavior of basalt-reinforced epoxy composites modified with biomass-derived seashell powder. *Biomass Convers Biorefin* 2024;14:26281–91.
14. Kumar A, Dixit S, Singh S, Sreenivasa S, Bains PS, Sharma R. Recent developments in the mechanical properties and recycling of fiber-reinforced polymer composites. *Polym Compos* 2025;46:3883–908.
15. Dhandapani N, Megalingam A. Mechanical and sound absorption behavior of sisal and palm fiber reinforced hybrid composites. *J Nat Fibers* 2022;19:4530–43.
16. Anand raj MK, Muthusamy S, Panchal H, Ibrahim AMM, Alsoufi MS, Elsheikh AH. Investigation of mechanical properties of dual-fiber reinforcement in composite. *J Mater Res Technol* 2022;18:3908–15.
17. Suriyaprakash M, Nallusamy M, Shanjai KSR, Akash N, Rohith V. Experimental investigation on mechanical of Ramie, Hemp fiber and coconut shell particle hybrid composites with reinforced epoxy resin. *Mater Today Proc* 2023;72:2952–6.
18. Sivasankar GA, Karthick PA, Boopathi C, Brindha S, Nirmalraj RJT, Benham A. Evaluation and comparison on mechanical properties of abaca and hemp fiber reinforced hybrid epoxy resin composites. *Mater Today Proc* 2023. In press.
19. Sumesh KR, Ajithram A, Palanisamy S, Kavimani V. Mechanical properties of ramie/flax hybrid natural fiber composites under different conditions. *Biomass Conv Bioref* 2024;14:29579–90.
20. Arumugam S, Kandasamy J, Md Shah AU, Hameed Sultan MT, Safri SNA, Abdul Majid MS, et al. Investigations on the mechanical properties of glass fiber/sisal fiber/chitosan reinforced hybrid polymer sandwich composite scaffolds for bone fracture fixation applications. *Polymers* 2020;12:1501.
21. De Cicco D, Asaee Z, Taheri F. Use of nanoparticles for enhancing the interlaminar properties of fiber-reinforced composites and adhesively bonded joints A review. *Nanomaterials* 2017;7:360–89.
22. Beemkumar N, Subbiah G, Upadhye VJ, Arora A, Jena SP, Priya KK, et al. Thermal stability and flame-retardant properties of a basalt/kevlar fiber-reinforced hybrid polymer composite with bran filler particulates. *Results Eng* 2025;25:104207.
23. Turaka S, Reddy KVK, Sahu RK, Katiyar JK. Mechanical properties of MWCNTs and graphene nanoparticles modified glass fibre-reinforced polymer nanocomposite. *Bullet Mater Sci* 2021;44:194–208.
24. Kamatchi T, Saravanan R, Rangappa SM, Siengchin S. Effect of filler content and size on the mechanical properties of graphene-filled natural fiber-based nanocomposites. *Biomass Convers Biorefin* 2023; 13:11311–20.
25. Reddivari BR, Vadapalli S, Sanduru B, Buddi T, Vafaeva KM, Joshi A. Fabrication and mechanical properties of hybrid fibre-reinforced polymer hybrid composite with graphene nanoplatelets and multiwalled carbon nanotubes. *Cogent Eng* 2024;11:2343586.
26. Hminghlui L, Ashok KG, Raju M, Praveen Kumar A, Damodaran A. Experimental and numerical studies on the mechanical characteristics of timoho fiber epoxy composites with nanofiller addition. *Polym Compos* 2024;45:4093–106.
27. Ganapathy T, Ramasamy K, Suyambulingam I, Siengchin S. Synergetic effect of graphene particles on novel biomass-based Ficus benghalensis aerial root/flax fiber-reinforced hybrid epoxy composites for structural application. *Biomass Convers Biorefin* 2024; 14:20713–50.
28. Kamesh B, Gude R, Maddamsetty A, Kebede Kassa M, Kumar Singh L, Arumugam AB. Investigation of the mechanical, absorption, flammability and swelling properties of graphene filled sisal/glass fiber reinforced polymer hybrid nanocomposites. *Cogent Eng* 2024;11: 2342433.
29. Oun A, Alajarmeh O, Manalo A, Abousnina R, Gerdes A. Durability of hybrid flax fibre-reinforced epoxy composites with graphene in hygrothermal environment. *Constr Build Mater* 2024;420:135584.
30. Dhilipkumar T, Venkatesan R, Kim SC, Murali AP, Shankar KV, Almutairi TM, et al. Assessing the structural and free vibrational performance of areca/ramie fibre composite reinforced with graphene nanofiller. *Ind Crops Prod* 2024;222:119599.
31. de Mendonça Neuba L, Silva TT, Reis LM, Monteiro SN, Simonassi NT, Candido LC, et al. Mechanical properties of sedge fiber-reinforced epoxy composites incorporated with graphene oxide. *J Mater Res Technol* 2025;34:1424–35.
32. Azka MA, Sapuan SM, Zainudin ES. Water absorption properties of graphene nanoplatelets filled bamboo/kenaf reinforced polylactic acid hybrid composites. *Int J Biol Macromol* 2025;285:138411.
33. Lapčík L, Sepetcioglu H, Murtaja Y, Lapčíková B, Vašina M, Ovsík M, et al. Study of mechanical properties of epoxy/graphene and epoxy/halloysite nanocomposites. *Nanotechnol Rev* 2023;12:2020520.
34. Mohanty AK, Misra M, Drzal LT. Surface modifications of natural fibers and performance of the resulting biocomposites: an overview. *Compos Interfaces* 2001;8:313–43.
35. Soundhar A, Kandasamy J. Mechanical, chemical and morphological analysis of crab shell/sisal natural fiber hybrid composites. *J Nat Fibers* 2021;18:1518–32.
36. Jayabal S, Sathiyamurthy S, Loganathan KT, Kalyanasundaram S. Effect of soaking time and concentration of NaOH solution on mechanical properties of coir-polyester composites. *Bull Mater Sci* 2012;35:567–74.
37. Hosseini A, Raji A. Improved double impact and flexural performance of hybridized glass basalt fiber reinforced composite with graphene nanofiller for lighter aerostructures. *Polym Test* 2023;125:108107.
38. Dhilipkumar T, Arunpandian M, Arumugam S, Sadeq AM, Karuppusamy P, Oh TH, et al. Exploring the synergistic effects of graphene on the mechanical and vibrational response of kenaf/pineapple fiber-reinforced hybrid composites. *Polym Compos* 2025;46:4591–604.
39. Sasi Kumar M, Sathish S, Makesh Kumar M, Gokulkumar S. Experimental studies on water absorption and mechanical properties of Hibiscus sabdariffa (roselle) and Urena lobata (caesar weed) plant fiber-reinforced hybrid epoxy composites: effect of weight fraction of nano-graphene fillers. *Int Polym Process* 2024;39:59–69.
40. Ashok KG, Kalaichelvan K, Anbarasu KG. Experimental studies on high-velocity impact of sandwich luffa/kevlar fiber epoxy composites with nanofiller inclusion. *Polym Bullet* 2024;81:12199–220.